SUSTAINED LOCAL DELIVERY OF SIRNA

FROM AN INJECTABLE SCAFFOLD

By

Christopher Edward Nelson

Thesis

Submitted to the Faculty of the

Graduate School of Vanderbilt University

in partial fulfillment of the requirements

for the degree of

MASTER OF SCIENCE

in

Biomedical Engineering

December, 2011

Nashville, Tennessee

Approved:

Professor Craig L. Duvall

Professor Scott A. Guelcher

To my wife, Heather, who is infinitely supportive

and my family, Leslie, Candace, Alexander, and Spencer who

fostered a desire for exploration and education

ACKNOWLEDGMENTS

TABLE OF CONTENTS

Appendix

LIST OF FIGURES

CHAPTER I

INTRODUCTION

Wound Healing

Chronic skin wounds represent a significant clinical burden, especially in diabetic patients whose skin wounds can become ulcerated and even lead to limb amputation. The current state of the art in biologic drugs for improving wound healing is Johnson and Johnson's Regranex®, one of the only clinically effective biologic drugs, which delivers platelet-derived growth factor significantly improving wound healing, but unfortunately cannot close 50% of chronic wounds [1]. Recently, small interfering RNA (siRNA) has been proposed as a potential treatment for a range of pathologies including skin wounds, and biomaterial scaffold-based siRNA delivery has been recently sought using both natural and synthetic scaffolds [2-5].

Non-healing diabetic skin wounds are characterized by a heightened and unresolved inflammatory phase leading to chronic ulceration. Because specific inflammatory mediators integral to this phenotype have been identified, siRNA may be a strong candidate drug for the treatment of chronically inflamed ulcers through sequence-specific gene silencing. By silencing pro-inflammatory genes (for example, p53, and Smad3 silencing have previously been attempted to improve wound healing) [4, 5] the wound site may be transformed into a more reparative environment that enables progression from the prolonged inflammatory phase and into remodeling and wound closure.

siRNA Discovery and Mechanism

Controlled manipulation of gene expression using RNA interference (RNAi) has been rigorously pursued for almost two decades now, and thorough elucidation of this mechanism combined with recent breakthroughs in RNA delivery technologies have RNAi poised to make a tremendous impact. The initial discovery of RNAi came in 1990 when Napoli et al. observed an unexpected reduction in expression when delivering RNA in an attempt to overexpress chalcone synthase in Petunias [6]. Others elucidated and applied this finding by delivering antisense

oligodeoxynucleotides (ODN), complementary sequences of DNA, which yielded modest reduction in gene expression in C. elegans [7]. In 1998, Fire *et al.* showed that intracellular-acting double stranded RNA (dsRNA) was more effective than either the sense or anti-sense strand alone [8]. In fact, dsRNA has been shown to be 100 to 1000 times more effective than ODNs due to a longer half-life and greater potency [9]. Over the next few years, researchers proved that endogenous RNAi, known as microRNA (miRNA), exist and that it serves as a natural, post-transcriptional controller of gene expression where cellular machinery selectively degrades complementary mRNA in an enzymatic manner [10]. The elucidation of similar machinery for RNAi in mammalian cells further heightened the interest in therapeutically harnessing these pathways [11].

Since these early findings, the mechanisms of ODN and that of miRNA, dsRNA, siRNA, and short hairpin RNA (shRNA) have been more clearly elucidated (see **Fig. 1**). Single-stranded antisense ODN are thought to function by multiple mechanisms including translational arrest due to steric blockage of ribosomes by ODN-mRNA Watson-Crick base pairing and also through RNase-H-mediated cleavage of both the ODN and mRNA strands [12]. Endogenous RNAi molecules in the form of microRNA (miRNA) enter the cytoplasm after transcription, or alternatively, functionally-similar dsRNA can be exogenously delivered. shRNA that more closely mimic the structure of endogenous miRNA have also been exogenously delivered [13]. In each of these cases, the RNase III family enzyme Dicer cleaves the miRNA/dsRNA/shRNA to produce guide RNA, more commonly known as small interfering RNA (siRNA). siRNA are double-stranded RNA 19-21 base pairs in length with 3' nucleotide overhangs [14], these molecules can assemble into the RNA induced silencing complex (RISC), a nuclease complex that degrades complementary mRNA in a sequence specific, enzymatic manner [10]. RNAi efficiency has been further improved by delivering siRNA that directly enters the RISC rather than upstream dsRNA/shRNA that must be processed first by Dicer [15].

These favorable properties of siRNA have led to rapid advancement into clinical tests for a variety of conditions including respiratory syncytial virus infection, macular degeneration, hepatitis B, renal failure, macular oedema, pachyonychia congenital, and solid tumors [16-18].
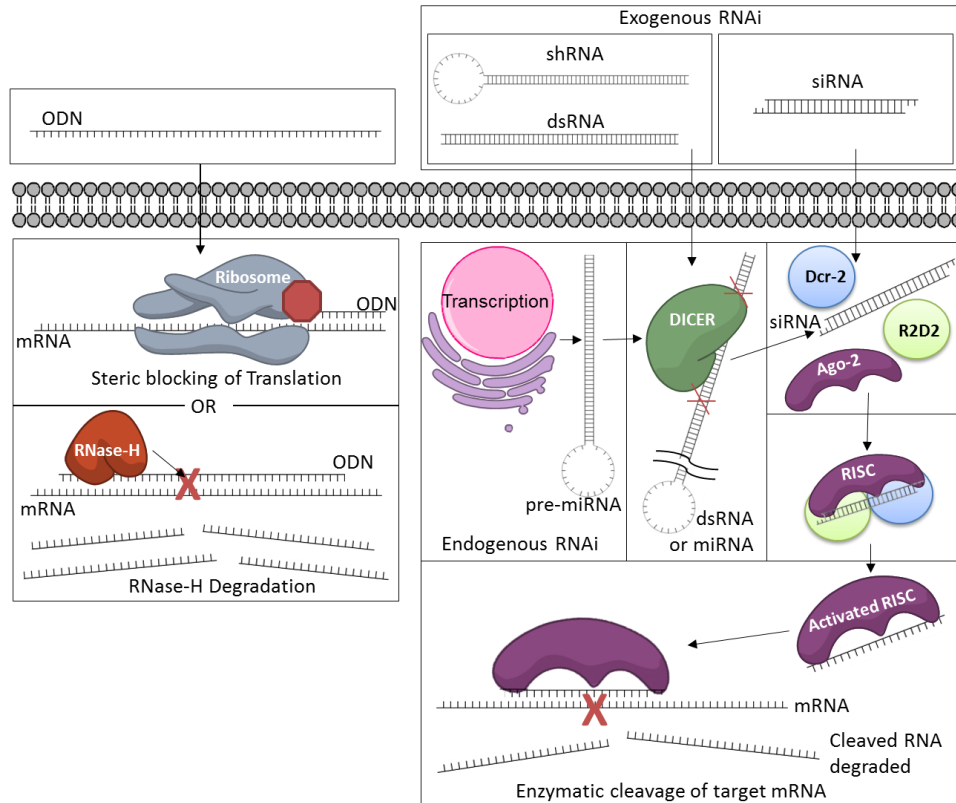
Figure 1 – RNAi mechanism: Mechanisms of RNA Interference (A) ODN silencing is believed to be induced by sterically blocking translation through hybridization with mRNA and RNAse-H mediated degradation of both the ODN and mRNA (B) Proposed mechanisms for RNA interference by miRNA, shRNA, dsRNA, and siRNA. Endogenous miRNA, which is made transcriptionally, and exogenously delivered shRNA/dsRNA must all be first processed into siRNA, double stranded RNA molecules around 20 base pairs in size. Exogenous siRNA can also be delivered that circumvents the need for dicer processing. siRNA is loaded onto the RISC complex and mediates degradation of mRNA complementary to the antisense siRNA strand. For each type of therapeutic RNAi, the exogenous RNA must reach the cytoplasm to interact with mRNA and other intracellular machinery required for gene silencing.

Smart Delivery

siRNA is regarded to have untapped clinical potential, but one of the major challenges to harnessing RNA interference pharmaceutically is efficient cytoplasmic delivery of the siRNA biomacromolecules into target cells. "Naked" siRNA has a very short half-life in vivo due to rapid degradation by nucleases and clearance through kidney filtration. siRNA is also relatively large molecular weight, anionic, and polar, making it impermeable to cell membranes. This is problematic for initial cellular internalization and for escape from endo-lysosomal vesicles following uptake by endocytosis. Thus, siRNA carriers are required that can both package and protect the siRNA and

deliver siRNA into the cytoplasm of the cell where the RISC machinery is located. Polycations have been heavily studied as an approach to package and protect siRNA and enable endosome escape via the proton sponge effect. However, most polycations are characterized by cytotoxicity and instability in vivo, and recent efforts have aimed to overcome these limitations.

Sustained Delivery

Although siRNA activity is catalytic, it does have a finite half-life in the cell. Previous reports generally note maximum silencing at around two days post-transfection [19] with normal gene expression restored by approximately one week in rapidly dividing cells [20]. One approach to extend silencing may be to achieve sustained, local release from scaffolds injected or transplanted onto the wound. Mostly natural materials such as alginate, collagen, and agarose have been pursued for biomaterial-based siRNA delivery to this point [2-5]. Recently, key proof-of-concept studies were published describing effective topical siRNA gene silencing in vivo using agarose scaffolds loaded with siRNA packaged into the commercial transfection reagent Lipofectamine 2000. This particular approach represents a significant breakthrough, though it did suffer from the potential limitation of siRNA diffusing from the scaffold in a relatively rapid "burst" release that required removal and re-application of siRNA-loaded scaffolds to achieve better and more sustained siRNA activity [4, 5]. It may be possible to achieve more optimal wound therapies with delivery systems that integrate efficient, nontoxic siRNA carriers into an injectable delivery matrix that can achieve sustained and tunable rates of siRNA release for greater than 1 week.

Approach

Currently, there are no commonly-utilized clinical applications of intracellular-acting biomacromolecular drugs (i.e., growth factors act on extracellular receptors). The delivery requirements for intracellular-acting biomolecules like siRNA are more rigorous because they cannot cross cellular membranes, and when endocytosed, the predominant fate is enzymatic degradation in lysosomes or recycling and extracellular clearance. Here, we describe a "smart" polymer carrier that "recognizes" environmental changes to become membrane disruptive in the lower pH environment of

4

endosomes. This innovative approach to gene inhibition may enable a new level of pharmaceutical breadth and specificity that would overcome many of the shortcomings of small molecule drugs and also allow manipulation of intracellular targets that were previously considered "undruggable". The majority of recent applications of siRNA have focused on in vitro validation, systemic in vivo delivery, or in vivo applications where siRNA formulations have been injected locally in saline with no regard for persistence of sustained bioactivity (i.e. intraocular or intratumoral injection, lung inhalation). The use of siRNA for regenerative applications could be tremendously enhanced by means for its sustained, local delivery from scaffolds that serve as porous tissue templates. The innovative combination of si-SPNs and PUR scaffolds provides a porous scaffold template for cell in-growth, ease of delivery for clinical applications (injectability), multiple levels of tunability for release kinetics, and ultimately, the ability to optimize siRNA activity for specific target genes and/or different pathological applications.

Here, we introduce a robust approach for siRNA delivery to skin wounds. This new platform incorporates siRNA delivering "smart" polymeric nanoparticles (**SPNs**) into injectable, biodegradable, porous, polyurethane (**PUR**)-based synthetic scaffolds.

CHAPTER II

SUSTAINED LOCAL DELIVERY OF SIRNA

FROM AN INJECTABLE SCAFFOLD

Introduction

The discovery of RNA interference [8] motivated extensive efforts toward harnessing gene-silencing biomacromolecules for clinical therapeutic use. Small-interfering RNA (siRNA) has rapidly advanced into clinical trials for indications such as macular degeneration [21], skin disorders [22], and targeted delivery to melanoma [18, 23, 24]. The current work focuses on development of a platform technology to be used for the controlled, local delivery for regenerative medicine, which is a less mature but promising application area for siRNA [25].

Effective delivery has been the primary limitation to more rapid and widespread adoption of siRNA for clinical use due to its susceptibility to nucleases and poor intracellular cytosolic delivery [26]. A variety of strategies have been developed to protect siRNA and improve intracellular delivery including electrostatic complexation with cationic lipids, polymers, and polysacaccharides, as well as conjugation to cell-penetrating/fusogenic peptides, dendrimers, antibodies, vitamins, and nanoparticles [27-37]. Controlled polymerization techniques such as reversible addition-fragmentation chain transfer (RAFT) polymerization offer a promising approach to designing synthetic polymers that are monodispersed, and contain spatially-defined functionalities [38, 39], and the current work employs a RAFT-synthesized, pH-responsive polymer-based micellar nanoparticle (si-NP) recently optimized for efficient and biocompatible intracellular siRNA delivery [40, 41].

The polyplex, bioconjugate, and nanoparticulate siRNA carriers that have advanced to *in vivo* preclinical testing have been primarily delivered intravenously or through local injection (i.e., intratumoral) in PBS. For tissue regeneration applications, it is anticipated that it will be desirable for siRNA activity to be locally sustained and mediated from a biocompatible and biodegradable tissue template. Because siRNA activity is typically transient and can be exhausted by one week in rapidly dividing cells [19, 20], natural materials including alginate, collagen and agarose have been applied

for sustained delivery of siRNA [2-5]. Pre-fabricated synthetic scaffolds made from ε-caprolactone and ethyl ethylene phosphate copolymer (PCLEEP) nanofibers have also been pursued for the release of siRNA/transfection reagent (*TransIT*-TKO) complexes and have been shown to achieve sustained delivery of bioactive siRNA for 28 days [42].

Porous, biocompatible, and biodegradable polyester polyurethanes (PUR) comprise a promising class of synthetic injectable biomaterials that can provide both mechanical support and also controlled drug release to regenerating tissues [43]. Several drugs, including insulin-like growth factor-1 (IGF-1), hepatocyte growth factor (HGF), basic fibroblast growth factor (bFGF), recombinant human bone morphogenetic protein 2 (rhBMP-2), platelet-derived growth factor (PDGF), and the antibiotic vancomycin have been incorporated into and delivered from PUR scaffolds [44-48]. Additionally, PURs support the ingrowth of cells in excisional cutaneous wounds [47] and bone defects [46, 48]. Further advantages of PURs are that they adhere to tissue, do not stimulate inflammation [47], and biodegrade into biocompatible side products at rates that can be tuned based on the polyester triol and isocyanate precursor compositions [49]. Importantly, the use of lysine-derived polyisocyanates in the PUR scaffolds makes them more clinically translatable because they can be synthesized using a two-component foaming process that allows a short manipulation time for filling of any shape or size defect, followed by rapid curing *in situ* [50, 51].

The current study pursues a novel application of PURs to deliver pH-responsive micellar si-NPs designed for the intracellular delivery of siRNA. This investigation validates homogenous loading of siRNA nanocarriers within the PUR scaffold, sustained, diffusion-controlled release of intact nanoparticles, and maintenance of gene silencing bioactivity of the released si-NPs.

Methods

Materials

All chemicals were purchased from Sigma-Aldrich (Milwaukee, WI, USA) except the following. Purchase of siRNA was from Applied Biosciences (Ambion), LDH cytotoxicity kit from Roche, Hiperfect transfection reagent (positive control) from Qiagen, and PD10 desalting columns

7

from GE healthcare. Lysine Triisocyanate (LTI) was purchased from Kyowa Hakko Kogyo Co., Ltd. (Tokyo, Japan). DMAEMA, and butyl methacrylate were vacuum distilled prior to use. 2,2'-Azobis(2-methylpropionitrile) (AIBN) was recrystallized twice with methanol.

Synthesis of 4-cyano-4-(ethylsulfanylthiocarbonyl) sulfanylvpentanoic acid (ECT)

The RAFT chain transfer agent ECT was synthesized following protocols previously described by Convertine et al. [40] adapted from Moad et al. [52]. Briefly, Ethanethiol (76 mmol, 4.72 g) was reacted with carbon disulfide (79 mmol, 6.0 g) in the presence of sodium hydride (79 mmol, 3.15 g) in diethyl ether for 1h. The resulting sodium S-ethyl trithiocarbonate was further reacted with iodine (25 mmol, 6.3 g) to obtain bis(ethylfulfanythiocarbonyl) disulfide, which was further refluxed with 4,4'-azobis(4-cyanopentanoic acid) in ethylacetate for 18 h. The crude ECT was purified by column chromatography using silica gel as the stationary phase and ethyl acetate:hexane (50:50) as the mobile phase. ^{1}H NMR (400MHz, CDCl$_3$): δ 1.36 t (SCH$_2$**CH$_3$**); δ 1.88 s (CCNC**H$_3$**); δ 2.3–2.65 m (**CH$_2$CH$_2$**); δ 3.35 q (SC**H$_2$**CH$_3$).

Synthesis of 2-propyl acrylic acid (PAA)

The synthesis of PAA was adapted from existing methods [53]. In brief, diethyl propylmalonate (200 mmol, 40.45 g) was stirred in 1M KOH in 95% ethanol and acifidied with HCl to yield 2-carbopropoxybutyric acid, which was reacted with diethylamine (200 mmol, 14.62 g) and formalin (200 mmol, 16.11 g) at room temperature for 24h, followed by reflux at 60°C for 8 hours. After acidification, the resulting 2 propylacrylate was refluxed in 2M KOH for 20 h to yield   2-propyl acrylic acid, which was extracted, dried, and vacuum distilled under vacuum to yield a colorless oil. ^{1}H NMR (400 MHz, CDCl$_3$) δ 0.97 t (**CH$_3$**CH$_2$); δ 1.55 m (CH$_3$**CH$_2$**CH$_2$); δ 2.31 t (CH$_3$CH$_2$**CH$_2$**); δ 5.69-6.32 q (**CH$_2$**=C); δ 12 s (CCOO**H**).

Synthesis and characterization of pDMAEMA macro CTA

The synthesis of the poly[2-(diethylamino)ethyl methacrylate] pDMAEMA macro chain transfer agent (mCTA) was conducted by RAFT polymerization using conditions adapted from [40].

Based on a polymerization kinetics experiments (**Appendix A**), the RAFT polymerization was conducted at 70 °C under a nitrogen atmosphere for eight hours with 1,4-dioxane as the solvent (70% by weight), an initial monomer to CTA ratio of 100, and a CTA to initiator ratio of 10. The pDMAEMA mCTA was isolated by precipitation into n-hexane (x3) and dried overnight. The polymer was analyzed by gel permeation chromatography (GPC, Shimadzu Crop., Kyoto, Japan) with an inline Wyatt miniDAWN TREOS light scattering detector (Wyatt Technology Corp., Santa Barabara, CA) and ^{1}H nuclear magnetic resonance spectroscopy (NMR, Bruker 400Mhz Spectrometer equipped with 9.4 Tesla Oxford magnet) for molecular weight and polydispersity.

Synthesis and characterization of DMAEMA-b-(PAA-co-BMA-co-DMAEMA)

RAFT polymerization was utilized to synthesize the second block as previously described [40]. Additional monomers butyl methacrylate (BMA), PAA, and DMAEMA were added to the pDMAEMA mCTA chain with an initial monomer to mCTA ratio of 250 in stoichiometric quantities of 50% BMA, 25% PAA, and 25% DMAEMA. The initiator AIBN was used with a mCTA to initiator ratio of 5. The polymerization was conducted for 18 hours under a nitrogen atmosphere at 70^oC. The resulting polymer was isolated by precipitation into chilled 50:50 ether:pentane, redissolved in acetone and precipitated into chilled pentane twice, and vacuum dried overnight. The polymer was then dissolved in a minimal amount of ethanol, diluted into dH_2O, and further purified using PD10 desalting columns (GE Healthcare). The eluent was frozen and lyophilized yielding a pure polymer powder. The polymer was analyzed by GPC for number average molecular weight (M_n) and polydispersity. NMR in $CDCl_3$ and D_2O was used to determine composition and verify the formation of micelles with a DMAEMA corona. Transmission Electron Microscopy (TEM, Philips CM20 Transmission Electron Microscope, EO, Netherlands) and Dynamic Light Scattering (DLS, Zetasizer nano-ZS Malvern Instruments Ltd, Worcestershire, U.K.) were used to confirm presence and size of micelles, to determine the critical micelle concentration, and to characterize micelle pH-responsiveness. Carbon TEM grids (Ted Pella Inc. Redding, CA) were spotted with 5uL of polymer solution (~50ug/mL) and dried under vacuum for 24 hours.

Formation and Characterization of siRNA-loaded Micellar Nanoparticles

siRNA was dissolved in nuclease free water, and si-NPs were formed by injecting siRNA in nuclease free polypropelene tubes, diluting with PBS, adding polymer in PBS, and incubating at room temperature for 30 minutes. si-NPs were formulated based on the charge ratio defined as the number of positively charged tertiary amines (assumed to be 50% at physiologic pH) on the DMAEMA block (N) to the number of negatively charged phosphate groups on the backbone of siRNA (P). Complexes were formed anywhere between 0.5 and 8 N/P. A 2% agarose gel was prepared with 0.5 µg/mL ethidium bromide and allowed to gel at room temperature. si-NPs and controls were run for 40 minutes at 100 V. This experiment was also conducted after pre-incubating the si-NPs in 50% serum to verify serum stability. Dynamic light scattering and ζ−potential were used for physicochemical characterization of the si-NPs, and TEM was used to further verify si-NP size and morphology.

Synthesis of si-NP-loaded PUR Scaffolds

Polyester triols were synthesized as previously described from a glycerol starter targeting 900 Da and a backbone comprising 60 wt% ε-caprolactone, 30 wt% glycolide, and 10 wt% D,L-lactide [47, 54, 55]. si-NPs were synthesized as described above using an N/P of 4 and 4 nmol of fluorescently labeled (6-FAM) siRNA against GAPDH or non-labeled siRNA with a scrambled sequence. si-NPs were frozen and lyophilized and the resulting powder was rigorously mixed into 134 µmol of the polyol component of PUR using a Hauschild DAC 150 FVZ-K SpeedMixer (FlackTek, Inc., Landrum, SC). A slight excess of lysine triisocyanate (387 µmol) was then added and scaffolds were allowed to cure at room temperature forming a porous PUR foam over approximately 10 minutes. 134 µmol of water was included in the polyol because it reacts with LTI to produce CO_2 which acts as a blowing agent and creates pores in the scaffold. The resulting 200 mg foams were sectioned into discs with a diameter of 13mm and a thickness of approximately 3mm.

PUR Characterization

Confocal microscopy (Zeiss LSM 510Meta) equipped with differential interference contrast (DIC) was used to analyze the distribution of si-NPs in the scaffold. The 13mm diameter by 3mm cylindrical foams were immersed in 1mL of PBS in a 24 well plate. Releasate was collected at regular intervals approximating an infinite sink condition, and release data were fit to the Weibull function [48, 56]. Releasate was analyzed by TEM and DLS for presence and size of released si-NPs.

Cell Culture and siRNA Knockdown

Mouse Embryonic Fibroblasts (NIH3T3) were cultured in Dulbecco's Modified Eagle's Medium (DMEM, Gibco Cell Culture, Carlsbad, CA) supplemented with 5% Bovine Calf Serum (BCS, Gibco), and 1% penicillin-streptomycin (Gibco). For gene silencing experiments, NIH3T3 mouse embryo fibroblasts were seeded at a density of 12,500 cells/cm^2 in a 12 well plate and allowed to adhere overnight. Fresh NPs or released NPs were added in fresh media with a final concentration of 6.25nM to 50nM siRNA and allowed to incubate for 24 hours. Each group was analyzed with n=3, and each replicate was run in triplicate during qRT-PCR. The cells were lysed and homogenized with QIAshredder (Qiagen), and RNA was purified using the RNeasy® Mini Kit (Qiagen). RNA quantity and quality was assessed with a nanodrop spectrophotometer ND-1000 (Thermo Scientific). cDNA was synthesized with iScript^{TM} cDNA synthesis kit (BIO-RAD) on a C1000^{TM} thermal cycler. Quantitative PCR was done using IQ^{TM} Real Time SYBR Green PCR Supermix on a quantitative thermal cycler (Bio-Rad iCycler iQ). GAPDH expression was normalized to β-Actin expression using the ΔΔCT method. Primers used were: β-actin Forward 5'-CTACGAGGGCTATGCTCTCCC-3', β-actin backward 5'-CGTCCTCATGCTACTCAGGCC-3', GAPDH Forward 5'-CTCACTCAAGATTGTCAGCAATG-3', GAPDH Backward 5'-GAGGGAGATGCTCAGTGTTGG-3'.

Imaging of Cell Uptake of si-NPs Post-release from PUR Scaffolds

NIH3T3s were seeded at 12,500 cells/cm^2 in 8 well chamber slides and incubated for 4 hours with FAM labeled siRNA containing si-NPs released from PUR scaffolds. The media was removed,

and the cells were washed 3x with PBS and fixed in 4% paraformaldehyde for 30 minutes. After 2 washes in PBS, cell nuclei were counterstained with Hoechst 33258 (5 µg/mL, Sigma) and then washed an additional 3x. Images were acquired on a fluorescent microscope.

Cytotoxicity

NIH3T3 cells were seeded at a density of 12,500 cells/cm^2 in a 96 well plate and allowed to adhere overnight. si-NPs were then added in fresh media and allowed to incubate for 24 hours. The cells were then lysed and analyzed for intracellular LDH with a Cytotoxicity Detection Kit (Roche Applied Science) as previously described [57], and a plate reader (infinite F500, Tecan Group Ltd., Mannedorf, Switzerland) set for absorbance at 492nm with reference at 595nm.

Statistical analysis

All data are reported as means ± standard error of the mean (SEM).   Analysis of Variance (ANOVA) was used to determine treatment effects and $p < 0.05$ was considered significant.

Polymer synthesis and characterization

4-cyano-4-(ethylsulfanylthiocarbonyl) sulfanylvpentanoic acid (ECT) was synthesized as previously described [40]. 2-propyl acrylic acid (PAA) was synthesized using established methods [53]. RAFT polymerization was used to synthesize a mCTA of DMAEMA (M_n = 11200g/mol, PDI = 1.40, (**Appendix B**). The pDMAEMA mCTA was used to polymerize a second block with a resultant M_n of 32040 g/mol for a total M_n of 43240 g/mol (PDI = 1.41) as shown in **Appendix B**. ^{1}H-NMR was used to confirm the percent composition of the second block which was determined to be 30%PAA, 25%DMAEMA, and 45%BMA (**Appendix C**). When dissolved in D_2O, ^{1}H-NMR peaks from the core-forming terpolymer are suppressed, verifying the formation of micelles in an aqueous environment. (**Appendix C**). The polymer structure is depicted in **Fig 2**.
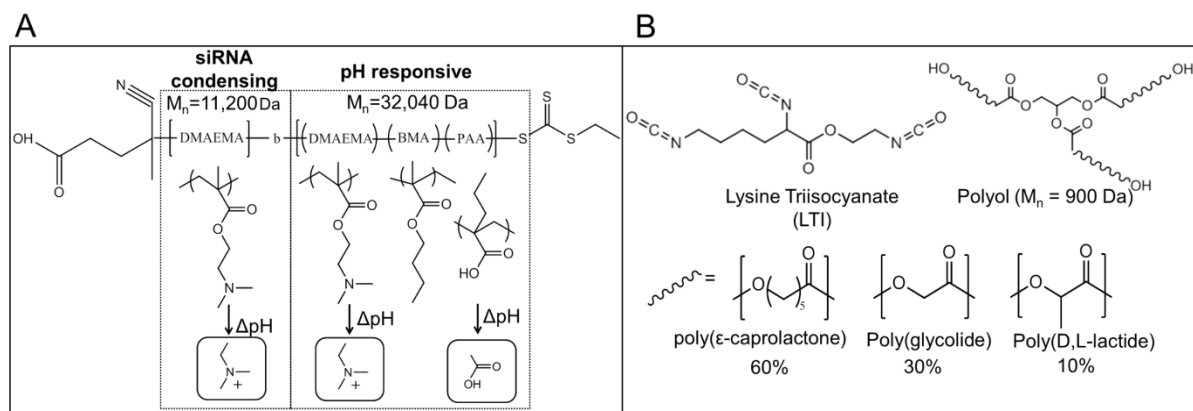
Figure 2 – Chemical composition of materials used for siRNA delivery: A) Chemical structure of the micelle-forming, pH–responsive diblock copolymer used for siRNA packaging and intracellular delivery. The homo-DMAEMA first block was designed for siRNA condensation due to the positive charge on the tertiary amines. The second block is pH-responsive and tuned for endosomal escape due to micelle destabilization and endosomolytic activity triggered by protonation of PAA and DMAEMA. B) Chemical structure of polyurethane precursors. LTI reacts with the –OH groups of the polyol to form urethane bonds and create the PUR network.

si-NP synthesis and characterization

Micellar nanoparticles were self-assembled in an aqueous environment and characterized for size and morphology by DLS and TEM respectively. TEM and DLS (**Fig 3**) report similar diameters of

31 nm and 39.6 nm respectively, with the smaller diameter seen with TEM being due to micelle

dehydration.

Figure 3 – Physicochemical characterization of freshly prepared and PUR-released si-NPs: **A)** Dynamic light scattering demonstrated that si-NP diameter was around 40-nm at N/P ratios of 2 or greater, and at N/P = 1, the charge neutrality caused the NPs to be less stable and larger. This is further represented by the $\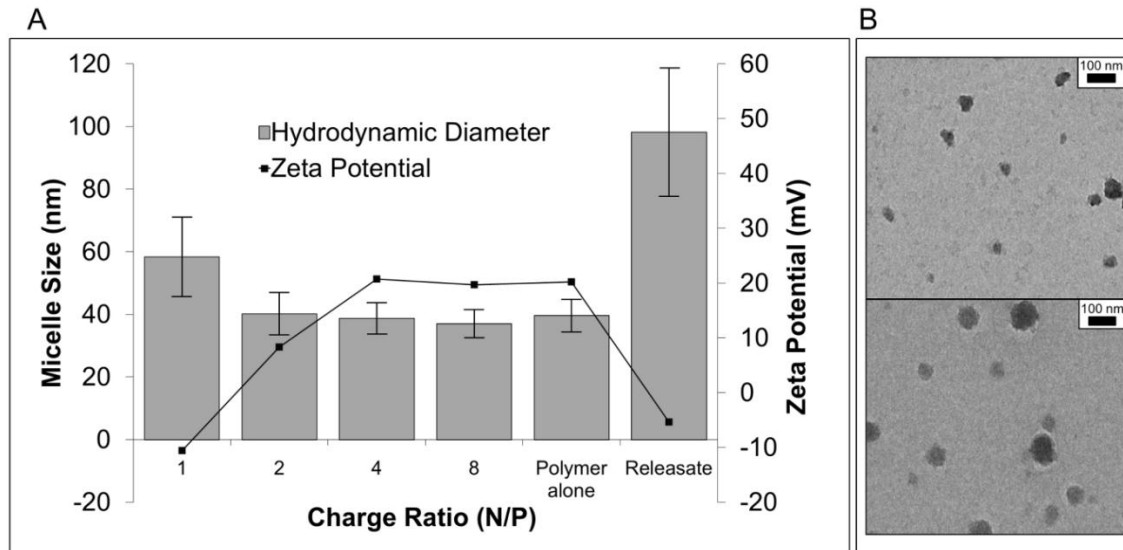zeta$–potential, which was slightly negative at N/P of 1, 8.3 mV at N/P of 2, and approximately 20 mV at all N/P of 4 or greater. **B)** The TEM image confirmed the micellar architecture and size of fresh si-NPs. Releasate si-NPs had a larger diameter of approximately 100 nm as shown both by DLS and TEM (B, bottom), and PUR-release si-NPs also had significantly reduced ζ–potential that was approximately charge neutral.

DLS of serially diluted samples revealed a critical micelle concentration (CMC) below 2 g/mL, based

on a DLS-detected loss of micelle stability (**Fig 4a**). DLS was also used to demonstrate the

dependency of the CMC on pH. The results confirm that micelle structure was destabilized at pH 5 at

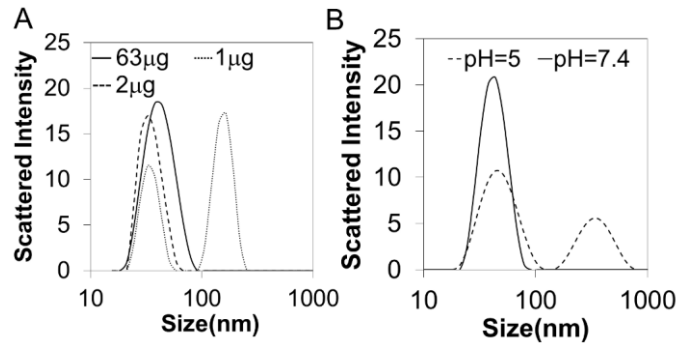a concentration of 100 μg/mL, which is important for micelle endosomolytic behavior (**Fig 4b**) [41].

Figure 4 – Micelle stability is dependent on concentration and pH: A) critical micelle concentration (CMC) determination using DLS demonstrated disruption of micelles occurred at 2 μg/mL. B) DLS also revealed pH-dependent destabilization of the micelles at pH = 5 at a concentration of 100 μg/mL.

Gel electrophoresis determined serum stable complexation of siRNA into si-NPs across a range of N:P ratios (**Appendix D**).

 si-NP-loaded PUR scaffolds

PUR foams were synthesized by reacting polyester triols (polyol) with lysine triisocyanate forming the porous polyurethane foam (**Fig 2b**). Differential interference contrast microscopy (DIC) of PUR scaffolds revealed an intact, connected porous structure (**Figure 5b,e**) with a mean pore diameter of 150μm ± 64μm. Confocal microscopy shows a relatively homogenous distribution of fluorescently labeled siRNA containing NPs throughout the PUR matrix (**Fig 5a-c**) comparable to the distribution seen in the PUR containing naked siRNA (**Fig 5d-f**).
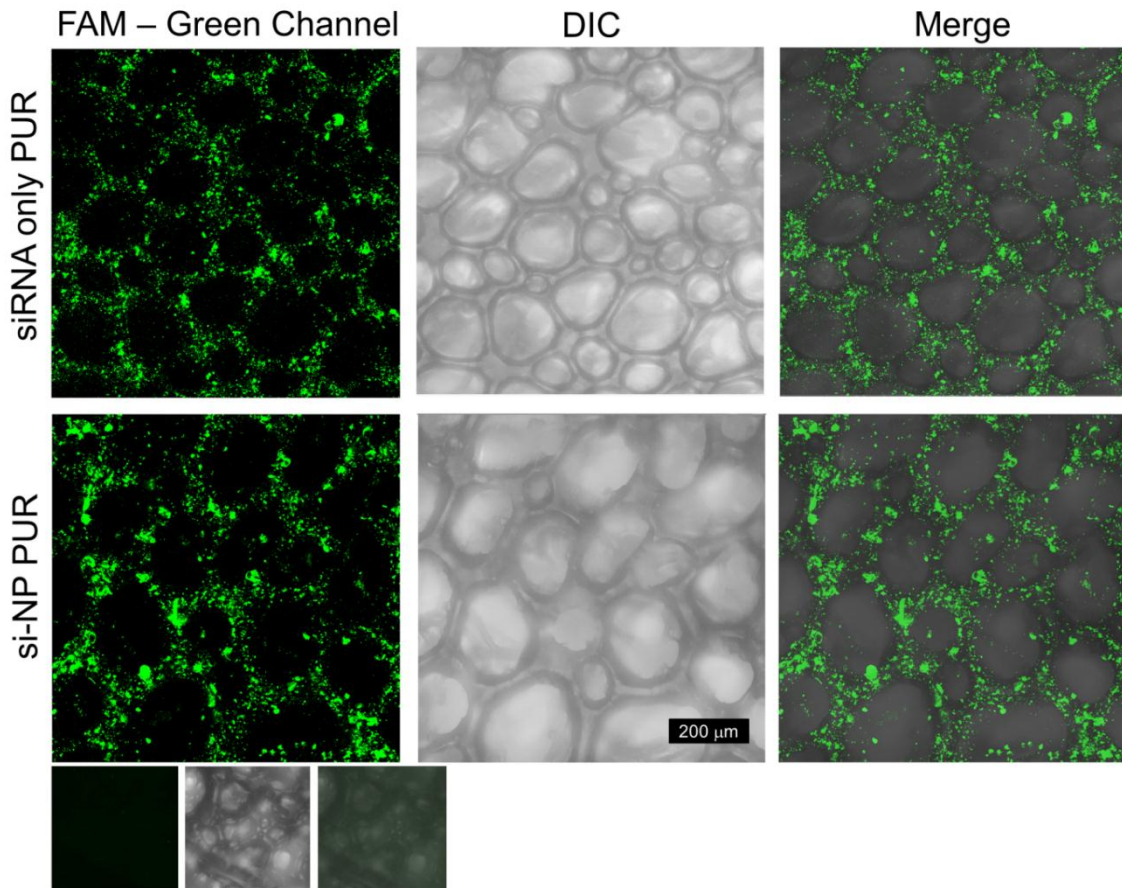
Figure 5 – FAM labeled siRNA and si-NPs distribution within the PUR scaffold:
Comparison of fluorescent confocal images of PUR scaffolds loaded with FAM-labeled siRNA or si-NPs. Row 1 is a scaffold loaded with naked siRNA. Row 2 is a scaffold loaded with si-NPs. The 3rd row is an empty scaffold to verify that there is no green auto-fluorescence of the PUR scaffold. Note that scaffold pores contain no fluorescence, and the distribution between naked siRNA and si-NPs is similar.

siRNA-NP Release Kinetics and Modeling

Release from the scaffold was quantitatively assessed using si-NPs made with fluorescently labeled siRNA.   Approximately 20% of the payload was released in the first 12 hours followed by a sustained release approaching 80% cumulative release by 21 days (**Fig 6**).
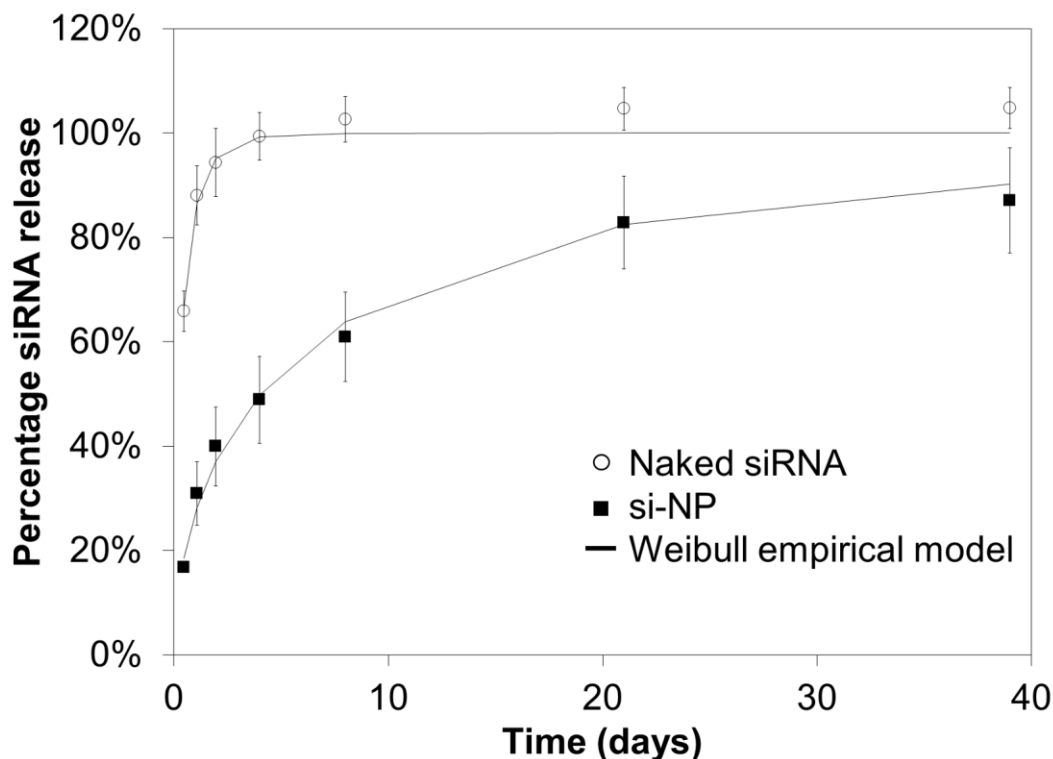
Figure 6 – Release of siRNA and si-NPs from PUR scaffolds is diffusion controlled: The Weibull empirical model equation best-fit was determined and is overlaid here for each data set.   Naked siRNA is rapidly released with an initial burst of over 60% at 12 hours and is entirely released by 3 days. si-NPs have a slower rate of release with a burst release of less than 20% during the first 12 hours, followed by sustained release that approaches 80% by 21 days.

Conversely, the much smaller naked siRNA diffuses from the scaffold much faster than si-NPs, reaching nearly 100% in 3 days. Importantly, TEM and DLS of releasate demonstrated that intact si-NPs, although of larger diameter than fresh si-NPs (approximately 100nm), were delivered from the PUR scaffolds (**Fig 2**).

The Weibull function has been previously used to evaluate the drug release mechanisms of drug eluting matrices that efficiently release their payload (cumulative release exceeding 60%) [48, 56]. The release of si-NPs was fit to the Weibull empirical model in Equation 1:

$$Eqn\ 1: \qquad \frac{M_t}{M_\infty} = 1 - \exp(-a \cdot t^b)$$

where M_t is the mass of si-NPs released at time t, M_∞ is the total mass of si-NPs, a is a constant

based on the system, and b is a constant based on the release kinetics. Previous reports suggest

that values of b < 0.75 indicate that Fickian diffusion is the dominant release mechanism [48, 56].

The values obtained from the best fit were found to be a=1.892, b=0.699, R^2=0.995 for siRNA only

and a=0.317, b=0.560, with R^2 = .996 for si-NPs.

For additional evidence supporting diffusion-controlled release of siRNA, we performed a

scaling analysis to compare the predicted and measured initial release rates. The Stokes-Einstein

equation (eqn 2) and the Higuchi equation [58] (eqn 3) were utilized together to further validate the

diffusion-controlled release mechanism. These equations, where D is the diffusivity, M_t is the rate of

mass transfer, and r is the radius of the particle, provide relationships that allow the initial mass

transfer rate to be related to the inverse of the square root of the radius of the solute:

$$Eqn\ 2: \qquad D \sim \frac{1}{r}$$

$$Eqn\ 3: \qquad M_t \sim \sqrt{D}$$

Assuming all conditions except hydrodynamic diameter are maintained constant between the

two samples except yields the following scaling prediction:

$$Eqn\ 4: \quad \frac{M_{siRNA}}{M_{si-NP}} = \frac{\sqrt{r_{si-NP}}}{\sqrt{r_{siRNA}}}$$

This analysis was completed assuming a hydrodynamic diameter of 2.56 nm for the siRNA,

which was the value suggested by Barone et al for a 28 mer duplex RNA [59]. The hydrodynamic

diameter of 38.69 nm that was experimentally determined using DLS for a charge ratio of 4/1 for si-

NPs was used. Based on the measured initial release of 17% for si-NPs and 66% for naked siRNA,

the left side of Eqn. 4 reduces to 3.88 and the right side 3.87. Thus the scaling anlyais is consistent

with the notion that the relase of siRNA from the scaffolds is governed by Fickaian diffusion.

PUR-released si-NP

Cytotoxicity experiments showed that the si-NPs were cytocompatible at the doses used

(**Appendix E**). Gene expression analyzed by qRT-PCR showed significant reduction (p<0.05) in

mRNA levels for GAPDH mediated by releasate collected between 0-24h, 24-48h, and 48-96h, while

controls containing scrambled siRNA showed no activity (**Fig 7a**). Further experimentation showed

that PUR-released si-NPs produced dose dependent silencing of GAPDH expression with the highest

dose of 50 nM producing approximately 50% gene knockdown (**Fig 7b**) while freshly prepared si-NPs

produced a dose dependent silencing with 83% reduction at 50nM. The finding that there was a

strong correlation between dose and gene silencing, indicated a siRNA dependent effect, and

importantly, scrambled siRNA controls had no observable activity. The microscopic observation of

diffuse fluorescent siRNA in the cytoplasm of cultured cells confirmed the maintenance of

endosomolytic behavior, cytoplasmic delivery, and bioactivity of the PUR-released si-NPs (**Fig 7c**).
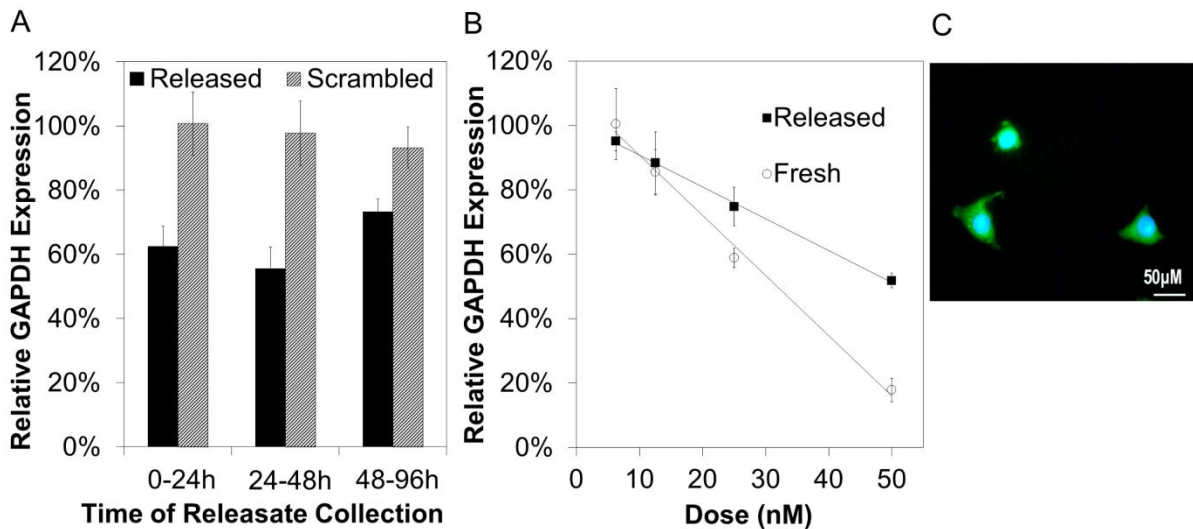
Figure 7 – Fresh and released si-NPs are delivered intracellularly and mediate gene specific silencing: qRT-PCR was used to measure expression of the model gene GAPDH relative to β-actin and then normalized to no treatment controls. A) Bioactivity of freshly prepared and PUR-released si-NPs collected during the defined timeframes 0-24h, 24-48h, and 48-96h indicates that bioactivity of si-NPs released from the PUR is not significantly altered over time. Statistical significance relative to scrambled control siRNA containing si-NPs was noted at all time points (p<0.05). B) Dose response of PUR-released si-NPs demonstrated a linear relationship (R^2= 0.999) between siRNA dose and silencing activity, suggesting an siRNA-dependent gene silencing effect. Minor reduction in siRNA bioactivity was apparent in PUR-released si-NPs relative to fresh si-NPs. C) Diffuse green fluorescence is noted in the cytoplasm of NIH3T3s after 4 hours of incubation with PUR-released si-NPs. This presence of FAM-labeled siRNA in the cytoplasm confirmed effective siRNA cytoplasmic delivery.

Discussion

Technologies that enable the efficient and sustained delivery of siRNA are a high-impact but relatively unmet need. This is primarily due to the number and complexity of the delivery barriers that exist. Here, a new platform is presented that is capable of both sustained and effective delivery of siRNA from a PUR scaffold capable of providing a biocompatible and biodegradable tissue template that can be cured *in situ* using a clinically-translatable injectable formulation. Due to nuclease susceptibility and membrane impermeability of naked siRNA, little success has been found with carrier-free siRNA delivery methodologies, and thus, the siRNA was first loaded into the pH-responsive micellar si-NPs prior to formulation with the biomaterial matrix.

The RAFT synthesized polymer shown in **Fig 2A** is the basis for the si-NPs and was specifically designed for improved cytoplasmic uptake, siRNA protection, and endosome escape [40, 41]. Toxicity of typically-utilized polyplexes made with cationic polymers [60] and the limitations associated with inefficient bioactivity due to lysosomal degradation or extracellular clearance [61] motivated the development of the polymer. si-NPs are formulated at positive charge ratios (typically 4:1) providing a net positive charge which facilitates efficient cell uptake by most cell types [62, 63]. Once in the endosome, decreasing pH destabilizes the micelle structure due to protonation of PAA and DMAEMA monomers and exposes the membrane-disruptive core [64]. The configuration of the second block (**Fig. 2A**) is finely tuned to provide a sharp pH response at the desired pH by incorporating appropriate amounts of hydrophobic BMA [65] and pH responsive DMAEMA and PAA. **Fig 4B** confirmed the pH-dependent micelle destabilization using DLS and it is hypothesized that this destabilization allows the hydrophobic 2nd block to penetrate and disrupt endosomal membranes and facilitate siRNA delivery to the cytoplasm [66-69]. Once internalized, siRNA may be competitively dissociated from the polymer through interactions within the cytoplasm by other ionic molecules [62] thus gaining access to the RNAi machinery in the cytoplasm.

Recently, biomaterials have been pursued for sustained siRNA delivery, with natural materials such as alginate, collagen and agarose being mostly used in these applications due to their biocompatibility [2-5]. However, these natural materials generally lack tunability and have been limited to rapid burst release of siRNA. The best sustained delivery to date has been achieved using

PCLEEP nanofiber scaffolds, however, the manufacture of the scaffold requires complex equipment (electrospinning apparatus) and must be pre-made to a defined size and geometry [42]. Therefore, there still remains a significant need for a more clinically translatable biomaterial that can conform to tissue defects of varied sizes and shapes where it will cure *in situ* and deliver siRNA locally in a sustained manner.

PUR scaffolds provide multiple advantages as a biomaterial for controlled drug delivery to tissue defects for several reasons. PUR scaffolds can be easily adapted to be injectable making clinical use easier and requiring no additional fabrication equipment [50, 51]. After injection, PURs react *in situ* to form a biocompatible and biodegradable tissue scaffold with inter-connected pores that effectively serves as a template for cell influx and tissue formation and remodeling [47]. The mechanism of degradation includes hydrolytic degradation (on the order of months) and macrophage-mediated oxidative degradation by reactive oxygen species (ROS) secretion (on the order of weeks) that is ideal for the timescale of wound healing [49]. Finally, PUR has been shown to deliver biologics efficiently, typically delivering as much as 80% of the payload [46-48]. However, a previous study has reported that 50-μm PLGA microspheres with rhPDGF bound to the surface supported <10% release over 21 days, suggesting that primary amines in the protein reacted with the polyisocyanate, resulting in loss of activity [47]. The present study has confirmed for the first time that nanoparticulate carriers incorporated in reactive PUR scaffolds support high-efficiency, diffusion-controlled release as seen in **Fig 6**. The release data demonstrates cumulative release of si-NPs approaching 80% over 21 days compared to naked siRNA which was released rapidly, approaching 100% delivery of the payload in three days. The mechanism of release for both free siRNA and si-NPs was found to be diffusion-controlled based on the Weibull model. Further, scaling analysis with the Stokes-Einstein and Higuchi equations demonstrated that the initial release rates of siRNA and si-NPs scales appropriated to the hydrodynamic diameter of the solute. The diffusion-based release suggests that an additional level of control exists by altering si-NP diffusivity in the PUR matrix to tune the rate of release by varying the nanoparticle size.

It is hypothesized that, in many applications, sustained delivery of siRNA into tissue defects will be ideal for producing a therapeutic effect since siRNA produces relatively transient gene

silencing activity [70]. It is hypothesized that when the formulation tested here is translated *in vivo*, the initial burst release will establish gene silencing while the continual, slower siRNA delivery over the next few weeks will sustain the initial effect over a few weeks. Importantly, several approaches exist for tuning PUR-based drug delivery to be more rapid or more sustained [46].

Fig 7A demonstrates that the activity of released NPs is not significantly reduced over the time frames tested (0-24, 24-48, 48-96 hours). Sustained delivery of active complexes is critical to compensate for transiency of siRNA in a highly proliferative environment (i.e. tissue regeneration). **Fig 7B** demonstrates that the siRNA-mediated reduction in GAPDH of PUR-released si-NPs is dose dependent. However, it is evident that there is partial loss of bioactivity post-release from the scaffold compared to fresh si-NPs. It is possible that this reduction in silencing is due to reorganization of the micelle structure or a partial si-NP aggregation during lyophilization and incorporation into the PUR. There was a detectable difference in size revealed by TEM and DLS (**Fig 3**) of fresh micelles versus PUR-released micelles, and the ζ-potential of PUR-relesate si-NPs was also found to be reduced. It could also be possible that unreacted components in the PUR specifically adsorb to the surface of the released si-NPs, thereby reducing the ζ-potential of the si-NPs resulting in aggregation. Our unpublished data have shown that 1-2% of the PUR mass leaches from the reactive material during the first 45 minutes of cure when incubated in serum medium. The primary components in the leachates include polyester triol, dipropylene glycol, and triethylene diamine. Hydrolytic degradation of the cured scaffolds releases α-hydroxy acids [49], which could bind electrostatically to the positive surface of the si-NPs. However, further studies will be necessary to better understand and overcome the alteration of the si-NPs during processing, and excipients such as agarose and sucrose may provide one route for improving their stability during lyophilization [71].

Conclusions

Injectable poly(ester urethane) foams were successfully utilized for sustained release of bioactive si-NPs for an extended period of 21 days. The si-NPs synthesized using RAFT were found to remain intact and bioactive following incorporation into and release from PUR scaffolds, although changes in si-NP size and bioactivity were evident relative to fresh si-NPs. As a platform technology,

the combination of PUR scaffolds and pH-responsive micellar siRNA carriers provides a logical

approach to basic scientific studies of long-term siRNA-mediated gene silencing at local, pathological

or healing tissue sites. The described system also has the potential to be applied to control cell

phenotype and fate in tissue constructs developed *in vitro*. Finally, as a therapeutic, the described

approach may be applied to reduce expression of deleterious genes and improve regeneration in

tissue defects.

CHAPTER III

FUTURE DEVELOPMENTS OF INTEREST

Optimization of Release

Based on the work presented in Chapter II, optimization of the quantity and quality of si-NPs is required. The mechanism of release from scaffold has been determined to be fickian diffusion, but details about the inclusion of si-NPs into the PUR scaffold are somewhat unclear. It is known that inclusion of PBS salts assists release. A better controlled system may utilize excipients that condense around si-NPs and covalently bind to the scaffold during synthesis [71]. These excipients may protect the structure, provide efficient release, and maintain their bioactivity. Encapsulation in PLGA microspheres may provide an additional method of controlling release [46].

Further Degrees of Control

Adding additional functionality to the polymers may improve the activity upon release and may add provide an additional means of control. Methods of stabilizing the polymers through preparation may maintain activity. Moieties that assist in siRNA release may improve activity once present inside the cell. Also, on-demand release of active complexes could improve wound healing by releasing active si-NPs only when the wound environment is over-expressing inflammatory signals. This may include a self-catalyzed hydrolytically degradable cation that can more efficiently unpacks and releases siRNA [72]. Reducible cationic polymers containing dithiols may have a similar effect by releasing siRNA when in the reducing environment of the cytoplasm in the presence of glutathione. Micelle crosslinking provides a remarkable way of increasing the stability of micelles through the processing into PUR scaffolds and can provide an additional means of controlled release [73]. A pH-responsive cross-linked micelle would improve stability until delivered into endosomes where the pH-labile bonds would break. Similarly, reducible cross-linked micelles would only break apart once exposed to glutathione in the cytoplasm of cells making them more stable to delivery. Micelles may also be cross-linked with enzymatically degradable peptides. Lastly, micelles may be tethered to the

scaffold through covalent linkages that are degradable by any of the aforementioned mechanisms (intracellular pH, reactive oxygen species signaling, enzymatic activity, etc) for on-demand release. Finally, another potential future advance will be development of methods to achieve cell type-specific targeting of siRNA in the skin wound. For example, in hyperinflammatory wounds, one may be able to optimize therapeutic benefit and/or minimize nonspecific effects by targeting of siRNA specifically to leukocytic cell types.

<div align="center">Testing of siRNA targets in animal models</div>

Molecular biologists have made tremendous advances toward understanding the mechanistic control of wound healing. This body of work will help to identify a variety of genes whose silencing could be potentially sought in wound healing therapies. One future requirement will be to identify the most therapeutically useful target genes for different pathological situations (i.e, chronic wound vs. burn or trauma victim, etc.). The first animal model tested will be a mouse that constituitivly expresses luciferase such that longitudinal gene knockdown studies can be done in the same mouse. Next, reporter mice will be used that express luciferase upon stimulation through an NFκB promoter. This model will be key in showing a reduction in inflammatory signaling in the mouse wound. Finally, a study in diabetic mice may reveal an improvement in time to wound closure leading to a promising clinical application.

Appendix A: RAFT Kinetic Experiment
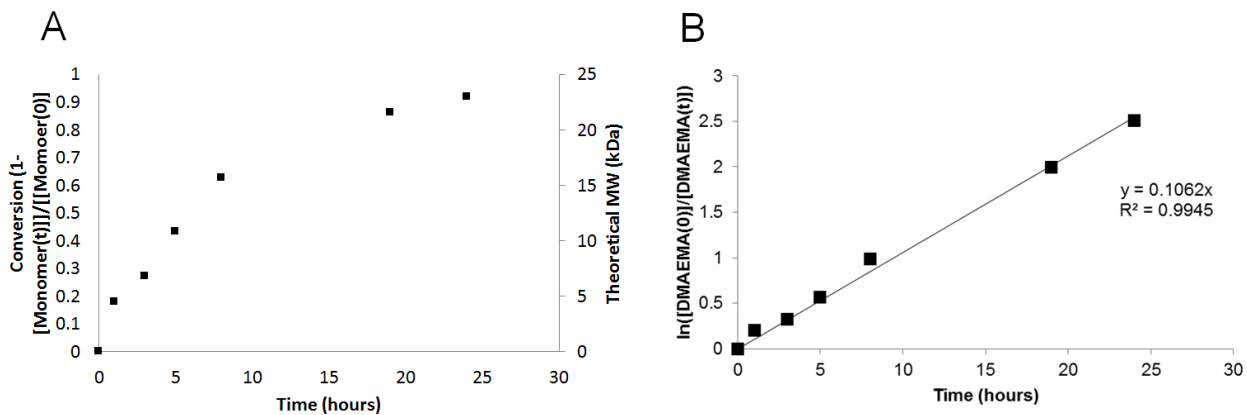
Supplementary Figure 1: RAFT kinetics study on polymerization of pDMAEMA mCTA. A) Conversion is initially linear and then begins to plateau. B) The log plot of the kinetics shows a linear first order polymerization kinetics. Eight hour polymerization time was selected for the desired block length and %conversion.

Appendix B: GPC Chromatograms
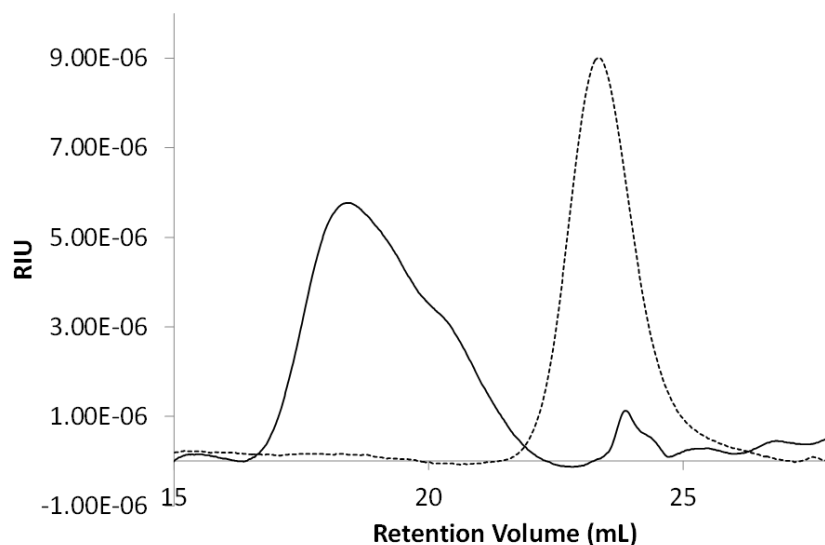
Supplementary Figure 2: Refractive Index traces from Gel Permeation Chromatography for macro CTA of DMAEMA (dotted line) and diblock copolymer (solid line)
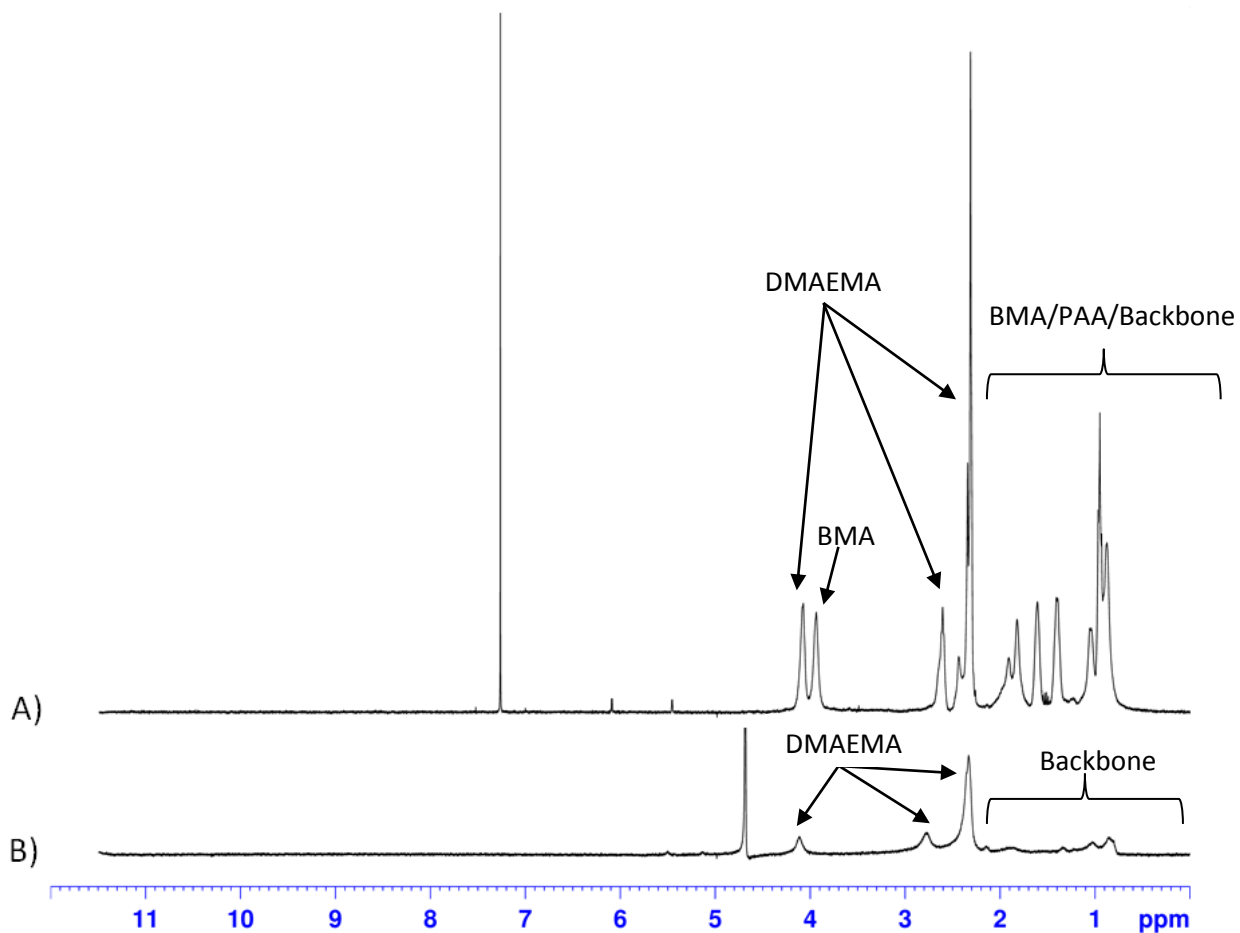
Supplementary Figure 3: ^{1}H NMR in CDCL$_3$ (A) and D$_2$O (B) demonstrates micelle formation. A) CDCL$_3$ spectrum has all peaks due to the good solvation of both blocks. B) Peaks in the hydrophobic block are suppressed due to the poor solvation. Peaks in the DMAEMA block show up the strongest.

Appendix D: Gel Retardation Assay
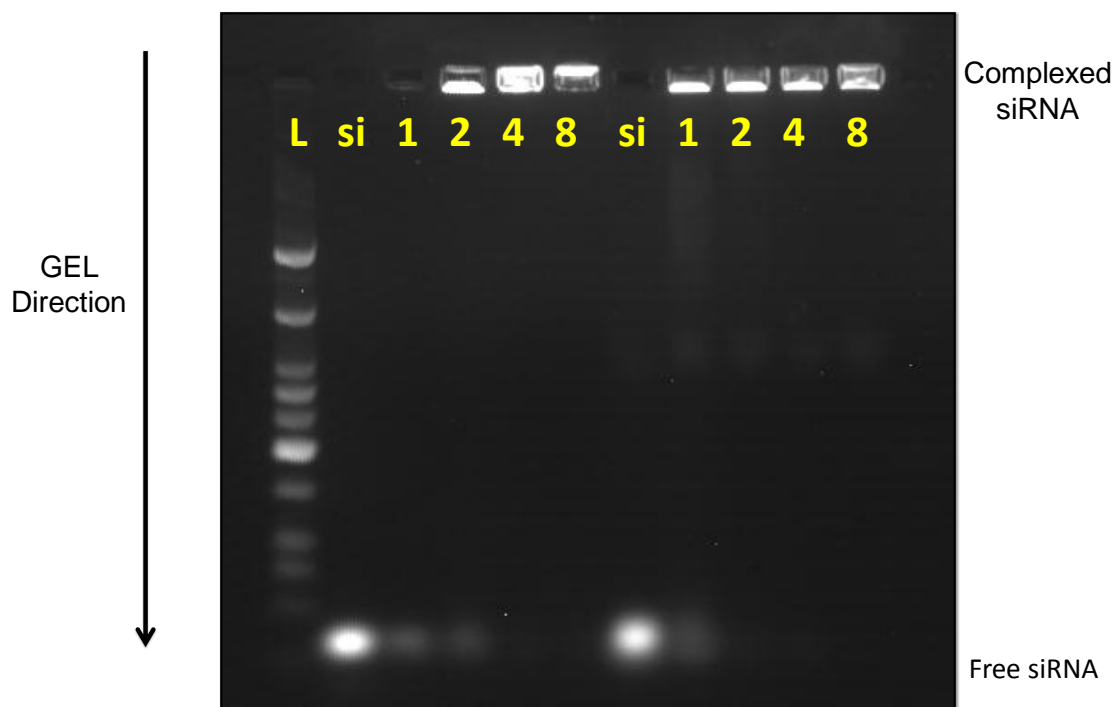
Supplementary Figure 4: si-NPs effectively complex siRNA and are serum stable. Gel electrophoresis of si-NPs formulated at varying charge ratios shown in yellow letters. The left half of the gel is in nuclease free water. The right half is completed in 50% Bovine Calf Serum proving stability to serum proteins. A charge ratio of 4:1 was utilized for further experimentation.

Appendix E: Cytotoxicity Assay
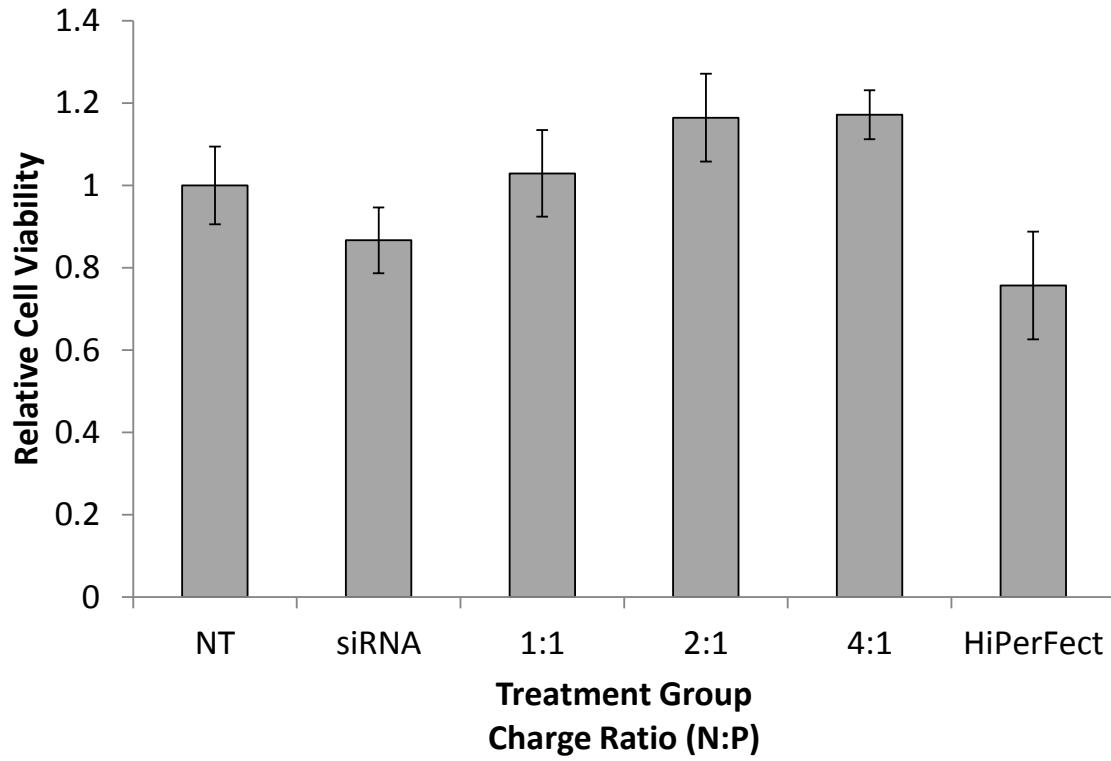
Supplementary Figure 5: Cytotoxicity profile of treatment groups shows minimal toxicity at the charge ratios used during this study.

REFERENCES

[1] Steed DL. Clinical evaluation of recombinant human platelet-derived growth factor for the treatment of lower extremity diabetic ulcers. Diabetic Ulcer Study Group. J Vasc Surg. 1995;21:71-8; discussion 9-81.

[2] Krebs MD, Jeon O, Alsberg E. Localized and Sustained Delivery of Silencing RNA from Macroscopic Biopolymer Hydrogels. Journal of the American Chemical Society. 2009;131:9204.

[3] Vinas-Castells R, Holladay C, di Luca A, Diaz VM, Pandit A. Snail1 down-regulation using small interfering RNA complexes delivered through collagen scaffolds. Bioconjug Chem. 2009;20:2262-9.

[4] Nguyen PD, Tutela JP, Thanik VD, Knobel D, Allen RJ, Chang CC, et al. Improved diabetic wound healing through topical silencing of p53 is associated with augmented vasculogenic mediators. Wound Repair and Regeneration. 2010;18:553-9.

[5] Lee JW, Tutela JP, Zoumalan RA, Thanik VD, Nguyen PD, Varjabedian L, et al. Inhibition of Smad3 expression in radiation-induced fibrosis using a novel method for topical transcutaneous gene therapy. Arch Otolaryngol Head Neck Surg. 2010;136:714-9.

[6] Napoli C, Lemieux C, Jorgensen R. Introduction of a Chimeric Chalcone Synthase Gene into Petunia Results in Reversible Co-Suppression of Homologous Genes in trans. Plant Cell. 1990;2:279-89.

[7] Guo S, Kemphues KJ. Par-1, a Gene Required for Establishing Polarity in C-Elegans Embryos, Encodes a Putative Ser/Thr Kinase That Is Asymmetrically Distributed. Cell. 1995;81:611-20.

[8] Fire A, Xu SQ, Montgomery MK, Kostas SA, Driver SE, Mello CC. Potent and specific genetic interference by double-stranded RNA in Caenorhabditis elegans. Nature. 1998;391:806-11.

[9] Bertrand JR, Pottier M, Vekris A, Opolon P, Maksimenko A, Malvy C. Comparison of antisense oligonucleotides and siRNAs in cell culture and in vivo. Biochem Bioph Res Co. 2002;296:1000-4.

[10] Hammond SM, Bernstein E, Beach D, Hannon GJ. An RNA-directed nuclease mediates post-transcriptional gene silencing in Drosophila cells. Nature. 2000;404:293-6.

[11] Elbashir SM, Harborth J, Lendeckel W, Yalcin A, Weber K, Tuschl T. Duplexes of 21-nucleotide RNAs mediate RNA interference in cultured mammalian cells. Nature. 2001;411:494-8.

[12] Vogl DT, Gewirtz AM. Nucleic Acid Therapies for Cancer Treatment. Totowa, N.J: Humana; 2008.

[13] Paddison PJ, Caudy AA, Bernstein E, Hannon GJ, Conklin DS. Short hairpin RNAs (shRNAs) induce sequence-specific silencing in mammalian cells. Genes Dev. 2002;16:948-58.

[14] Bernstein E, Caudy AA, Hammond SM, Hannon GJ. Role for a bidentate ribonuclease in the initiation step of RNA interference. Nature. 2001;409:363-6.

[15] Elbashir SM, Lendeckel W, Tuschl T. RNA interference is mediated by 21-and 22-nucleotide RNAs. Gene Dev. 2001;15:188-200.

[16] Zamora MR, Budev M, Rolfe M, Gottlieb J, Humar A, Devincenzo J, et al. RNA interference therapy in lung transplant patients infected with respiratory syncytial virus. Am J Respir Crit Care Med. 2011;183:531-8.

[17] Whitehead KA, Langer R, Anderson DG. Knocking down barriers: advances in siRNA delivery. Nat Rev Drug Discov. 2009;8:129-38.

[18] Davis ME, Zuckerman JE, Choi CHJ, Seligson D, Tolcher A, Alabi CA, et al. Evidence of RNAi in humans from systemically administered siRNA via targeted nanoparticles. Nature. 2010;464:1067-70.

[19] Layzer JM, McCaffrey AP, Tanner AK, Huang Z, Kay MA, Sullenger BA. In vivo activity of nuclease-resistant siRNAs. RNA. 2004;10:766-71.

[20] Dykxhoorn DM, Palliser D, Lieberman J. The silent treatment: siRNAs as small molecule drugs. Gene Ther. 2006;13:541-52.

[21] Kaiser PK, Symons RC, Shah SM, Quinlan EJ, Tabandeh H, Do DV, et al. RNAi-based treatment for neovascular age-related macular degeneration by Sirna-027. Am J Ophthalmol. 2010;150:33-9 e2.

[22] Leachman SA, Hickerson RP, Schwartz ME, Bullough EE, Hutcherson SL, Boucher KM, et al. First-in-human mutation-targeted siRNA phase Ib trial of an inherited skin disorder. Mol Ther. 2010;18:442-6.

[23] Davis ME. The first targeted delivery of siRNA in humans via a self-assembling, cyclodextrin polymer-based nanoparticle: from concept to clinic. Mol Pharm. 2009;6:659-68.

[24] Ribas A, Zuckerman JE, Hsueh T, Koya RC, Davis ME. siRNA Knockdown of Ribonucleotide Reductase Inhibits Melanoma Cell Line Proliferation Alone or Synergistically with Temozolomide. Journal of Investigative Dermatology. 2011;131:453-60.

[25] Yao Y, Wang C, Varshney RR, Wang DA. Antisense makes sense in engineered regenerative medicine. Pharm Res. 2009;26:263-75.

[26] White PJ. Barriers to successful delivery of short interfering RNA after systemic administration. Clin Exp Pharmacol Physiol. 2008;35:1371-6.

[27] Gao K, Huang L. Nonviral methods for siRNA delivery. Mol Pharm. 2009;6:651-8.

[28] Agrawal A, Min DH, Singh N, Zhu H, Birjiniuk A, von Maltzahn G, et al. Functional delivery of siRNA in mice using dendriworms. ACS Nano. 2009;3:2495-504.

[29] Convertine AJ, Benoit DS, Duvall CL, Hoffman AS, Stayton PS. Development of a novel endosomolytic diblock copolymer for siRNA delivery. J Control Release. 2009;133:221-9.

[30] Jafari M, Chen P. Peptide mediated siRNA delivery. Curr Top Med Chem. 2009;9:1088-97.

[31] Lee JS, Green JJ, Love KT, Sunshine J, Langer R, Anderson DG. Gold, poly(beta-amino ester) nanoparticles for small interfering RNA delivery. Nano Lett. 2009;9:2402-6.

[32] Nishina K, Unno T, Uno Y, Kubodera T, Kanouchi T, Mizusawa H, et al. Efficient in vivo delivery of siRNA to the liver by conjugation of alpha-tocopherol. Mol Ther. 2008;16:734-40.

[33] Qi L, Gao X. Quantum dot-amphipol nanocomplex for intracellular delivery and real-time imaging of siRNA. ACS Nano. 2008;2:1403-10.

[34] Watanabe K, Harada-Shiba M, Suzuki A, Gokuden R, Kurihara R, Sugao Y, et al. In vivo siRNA delivery with dendritic poly(L-lysine) for the treatment of hypercholesterolemia. Mol Biosyst. 2009;5:1306-10.

[35] Wu SY, McMillan NA. Lipidic systems for in vivo siRNA delivery. AAPS J. 2009;11:639-52.

[36] Xia CF, Boado RJ, Pardridge WM. Antibody-mediated targeting of siRNA via the human insulin receptor using avidin-biotin technology. Mol Pharm. 2009;6:747-51.

[37] Ghosn B, Kasturi SP, Roy K. Enhancing polysaccharide-mediated delivery of nucleic acids through functionalization with secondary and tertiary amines. Curr Top Med Chem. 2008;8:331-40.

[38] Moad G, Chiefari J, Chong YK, Ercole F, Krstina J, Jeffery J, et al. Living free-radical polymerization by reversible addition-fragmentation chain transfer: The RAFT process. Macromolecules. 1998;31:5559-62.

[39] Boyer C, Bulmus V, Davis TP, Ladmiral V, Liu J, Perrier S. Bioapplications of RAFT polymerization. Chem Rev. 2009;109:5402-36.

[40] Convertine A, Benoit D, Duvall C, Hoffman A, Stayton P. Development of a novel endosomolytic diblock copolymer for siRNA delivery. J Control Release. 2009;133:221-9.

[41] Convertine AJ, Diab C, Prieve M, Paschal A, Hoffman AS, Johnson PH, et al. pH-Responsive Polymeric Micelle Carriers for siRNA Drugs. Biomacromolecules. 2010.

[42] Rujitanaroj PO, Wang YC, Wang J, Chew SY. Nanofiber-mediated controlled release of siRNA complexes for long term gene-silencing applications. Biomaterials. 2011;32:5915-23.

[43] Guelcher SA. Biodegradable Polyurethanes: Synthesis and Applications in Regenerative Medicine. Tissue Engineering Part B: Reviews. 2008;14:3-17.

[44] Guan J, Stankus JJ, Wagner WR. Biodegradable elastomeric scaffolds with basic fibroblast growth factor release. J Control Release. 2007;120:70-8.

[45] Nelson DM, Baraniak PR, Ma Z, Guan J, Mason NS, Wagner WR. Controlled release of IGF-1 and HGF from a biodegradable polyurethane scaffold. Pharm Res. 2011;28:1282-93.

[46] Li B, Yoshii T, Hafeman AE, Nyman JS, Wenke JC, Guelcher SA. The effects of rhBMP-2 released from biodegradable polyurethane/microsphere composite scaffolds on new bone formation in rat femora. Biomaterials. 2009;30:6768-79.

[47] Li B, Davidson JM, Guelcher SA. The effect of the local delivery of platelet-derived growth factor from reactive two-component polyurethane scaffolds on the healing in rat skin excisional wounds. Biomaterials. 2009;30:3486-94.

[48] Li B, Brown KV, Wenke JC, Guelcher SA. Sustained release of vancomycin from polyurethane scaffolds inhibits infection of bone wounds in a rat femoral segmental defect model. J Control Release. 2010;145:221-30.

[49] Hafeman AE, Zienkiewicz KJ, Zachman AL, Sung HJ, Nanney LB, Davidson JM, et al. Characterization of the degradation mechanisms of lysine-derived aliphatic poly(ester urethane) scaffolds. Biomaterials. 2011;32:419-29.

[50] Adolph EJ, Hafeman A, Davidson J, Nanney L, Guelcher S. Injectable Polyurethane Composite Scaffolds Delay Wound Contraction and Support Cellular Infiltration and Remodeling in Rat Excisional Wounds. Journal of Biomedical Materials Research: Part A. (accepted).

[51] Hafeman AE, Li B, Yoshii T, Zienkiewicz K, Davidson JM, Guelcher SA. Injectable biodegradable polyurethane scaffolds with release of platelet-derived growth factor for tissue repair and regeneration. Pharm Res. 2008;25:2387-99.

[52] Moad G, Chong YK, Postma A, Rizzardo E, Thang SH. Advances in RAFT polymerization: the synthesis of polymers with defined end-groups. Polymer. 2005;46:8458-68.

[53] Ferrito M, Tirrell DA. Poly(2-ethylacrylic acid). Macromol Synth. 1992;11:59-62.

[54] Guelcher SA, Patel V, Gallagher KM, Connolly S, Didier JE, Doctor JS, et al. Synthesis and in vitro biocompatibility of injectable polyurethane foam scaffolds. Tissue Eng. 2006;12:1247-59.

[55] Guelcher S, Srinivasan A, Hafeman A, Gallagher K, Doctor J, Khetan S, et al. Synthesis, in vitro degradation, and mechanical properties of two-component poly(ester urethane)urea scaffolds: effects of water and polyol composition. Tissue Eng. 2007;13:2321-33.

[56] Papadopoulou V, Kosmidis K, Vlachou M, Macheras P. On the use of the Weibull function for the discernment of drug release mechanisms. International Journal of Pharmaceutics. 2006;309:44-50.

[57] Duvall CL, Convertine AJ, Benoit DS, Hoffman AS, Stayton PS. Intracellular delivery of a proapoptotic peptide via conjugation to a RAFT synthesized endosomolytic polymer. Mol Pharm. 2010;7:468-76.

[58] Siepmann J, Peppas NA. Higuchi equation: Derivation, applications, use and misuse. Int J Pharm. 2011;418:6-12.

[59] Barone F, Cellai L, Matzeu M, Mazzei F, Pedone F. DNA, RNA and hybrid RNA-DNA oligomers of identical sequence: structural and dynamic differences. Biophys Chem. 2000;86:37-47.

[60] Akhtar S, Benter IF. Nonviral delivery of synthetic siRNAs in vivo. J Clin Invest. 2007;117:3623-32.

[61] Medina-Kauwe LK, Xie J, Hamm-Alvarez S. Intracellular trafficking of nonviral vectors. Gene Ther. 2005;12:1734-51.

[62] Cho YW, Kim JD, Park K. Polycation gene delivery systems: escape from endosomes to cytosol. J Pharm Pharmacol. 2003;55:721-34.

[63] van der Aa MA, Huth US, Hafele SY, Schubert R, Oosting RS, Mastrobattista E, et al. Cellular uptake of cationic polymer-DNA complexes via caveolae plays a pivotal role in gene transfection in COS-7 cells. Pharm Res. 2007;24:1590-8.

[64] Jones RA, Cheung CY, Black FE, Zia JK, Stayton PS, Hoffman AS, et al. Poly(2-alkylacrylic acid) polymers deliver molecules to the cytosol by pH-sensitive disruption of endosomal vesicles. Biochem J. 2003;372:65-75.

[65] El-Sayed ME, Hoffman AS, Stayton PS. Rational design of composition and activity correlations for pH-sensitive and glutathione-reactive polymer therapeutics. J Control Release. 2005;101:47-58.

[66] Thomas JL, Barton SW, Tirrell DA. Membrane solubilization by a hydrophobic polyelectrolyte: surface activity and membrane binding. Biophys J. 1994;67:1101-6.

[67] Thomas JL, Tirrell DA. Polyelectrolyte-Sensitized Phospholipid-Vesicles. Accounts Chem Res. 1992;25:336-42.

[68] Borden KA, Eum KM, Langley KH, Tirrell DA. Interactions of Synthetic-Polymers with Cell-Membranes + Model Membrane Systems .13. On the Mechanism of Polyelectrolyte-Induced Structural Reorganization in Thin Molecular Films. Macromolecules. 1987;20:454-6.

[69] Hoffman AS, Lackey CA, Press OW, Stayton PS. A biomimetic pH-responsive polymer directs endosomal release and intracellular delivery of an endocytosed antibody complex. Bioconjugate Chem. 2002;13:996-1001.

[70] Krebs MD, Alsberg E. Localized, Targeted, and Sustained siRNA Delivery. Chem-Eur J. 2011;17:3054-62.

[71] Lei Y, Rahim M, Ng Q, Segura T. Hyaluronic acid and fibrin hydrogels with concentrated DNA/PEI polyplexes for local gene delivery. J Control Release. 2011.

[72] Truong NP, Jia Z, Burgess M, Payne L, McMillan NA, Monteiro MJ. Self-catalyzed degradable cationic polymer for release of DNA. Biomacromolecules. 2011;12:3540-8.

[73] Lee SJ, Min KH, Lee HJ, Koo AN, Rim HP, Jeon BJ, et al. Ketal cross-linked poly(ethylene glycol)-poly(amino acid)s copolymer micelles for efficient intracellular delivery of doxorubicin. Biomacromolecules. 2011;12:1224-33.